



# New generation of $\alpha$ -MnO<sub>2</sub> nanowires @PDMS composite as a hydrogen gas sensor

Seyedeh Mehri Hamidi<sup>1</sup> · Alireza Mosivand<sup>1</sup> · Mina Mahboubi<sup>1</sup> · Hadi Arabi<sup>2</sup> · Narin Azad<sup>2</sup> · Murtada Riyadh Jamal<sup>2</sup>

Received: 10 November 2017 / Accepted: 13 February 2018  
© Springer-Verlag GmbH Germany, part of Springer Nature 2018

## Abstract

New hydrogen gas sensor has been prepared by  $\alpha$ -MnO<sub>2</sub> nanowires in polydimethylsiloxane matrix. For this purpose, the high aspect ratio  $\alpha$ -MnO<sub>2</sub> nanowires has been prepared by the aid of hydrothermal method and then dispersed into poly-dimethyl siloxane polymer media. For gas sensing, the samples have been exposed under different gas concentrations from 0 to 5%. The sensor responses have been examined by normalized ellipsometric parameter with respect to the chamber filled with N<sub>2</sub> Gas. Our results indicate linear behavior of resonance wavelength in ellipsometric parameter as a function of gas concentrations which can open a new insight for the sample's capability to hydrogen gas sensing applications.

## 1 Introduction

Optically hydrogen gas sensors have been extensively studied due to the fast data recording and easy signal transportation. These sensors can be designed, and fabricated as miniaturized and multi-wavelengths heads to use in industrial fields such as rocket propellant, metallurgy, home appliances, and factory. These optical sensors can be classified into fields such as fiber optic sensors [1], interferometers [2], semiconductor [3], MEMS [4], surface state waves [5] and also thin absorptive film such as palladium (Pd) which can absorb 900 times of its volume get much attention in this field [6, 7].

In spite of metal thin films, the metal oxide gas sensors have been widely used in recent years. Among these metal oxide classes, manganese dioxide (MnO<sub>2</sub>) which depends on its crystalline phases can be used as an efficient energy storage in batteries [8], ion-exchanger [9], oxidizer [10] and also absorber [11]. The latest usage of these structures drift scientists to design and construct gas sensors such as hydrogen gas sensors [12]. Use of manganese dioxide components as a hydrogen gas sensor has been reported by many researchers

because of its cost and thermal stability characteristics. Based on these reports, the side-heated hydrogen gas sensor is based on high aspect ratio nanowires [13], potentiometric-type H<sub>2</sub> gas sensor [14], and MnO<sub>2</sub> nanoflake sensor [15].

For this purpose, compared to its bulk, powder or thin films structures, nanostructures of them as nanoparticles or one-dimensional nanostructures such as nanowires has attracted extensive attention because of the high surface to volume ratio [16]. Different structural forms of MnO<sub>2</sub> can be produced via various methods. The famous of these structures are  $\alpha$ ,  $\beta$ ,  $\gamma$  and  $\delta$ -MnO<sub>2</sub>, which differ from each other by the location of the MnO<sub>6</sub> octahedron. This displacement provides different void spaces in MnO<sub>2</sub> structures [17].

Controlling the parameters of synthesis methods will affect the dimension and size of the MnO<sub>2</sub> phases. One-dimensional structure of MnO<sub>2</sub>, as a critical factor, can provide various properties for individual applications. Therefore, well-controlled size and dimensionality of MnO<sub>2</sub> are very important. Although  $\alpha$ -MnO<sub>2</sub> nanostructures can be used as catalyst absorbents and Li+-related batteries [18], using these materials as a new generation of gas sensor has been examined for the first time in this report.

✉ Seyedeh Mehri Hamidi  
M\_hamidi@sbu.ac.ir

<sup>1</sup> Magneto-plasmonic Lab, Laser and Plasma Research Institute, Shahid Beheshti University, Tehran, Iran

<sup>2</sup> Renewable Energies, Magnetism and Nanotechnology Research Laboratory, Physics Department, Faculty of Science, Ferdowsi University of Mashhad, Mashhad, Iran

## 2 Experimental procedure

$\alpha$ -MnO<sub>2</sub> nanowires have been prepared by hydrothermal method using [MnSO<sub>4</sub>·H<sub>2</sub>O], [(NH<sub>4</sub>)<sub>2</sub>S<sub>2</sub>O<sub>8</sub>] and [(NH<sub>4</sub>)<sub>2</sub>SO<sub>4</sub>] as the starting materials. 0.02 mol of MnSO<sub>4</sub>·H<sub>2</sub>O and 0.02 mol of (NH<sub>4</sub>)<sub>2</sub>S<sub>2</sub>O<sub>8</sub> were dissolved in 42 ml

of deionized water. Then 0.08 mol of  $(\text{NH}_4)_2\text{SO}_4$  in 42 ml of deionized water was added to the initial solution. After mixing them with a stirrer at about 30 min, it was transferred into a Teflon-lined stainless steel autoclave and then reacted for 12 h at 120 °C. After this, the precipitation was rinsed for five times with deionized water and ethanol and finally dried at 80 °C for 12 h.

Powder X-ray diffraction (D8-Advance–Bruker using  $\text{Cu K}\alpha$  radiation with a step of 0.02 °/s) measurements were employed to identify the crystal structure of the  $\alpha\text{-MnO}_2$  samples. A field-emission scanning electron microscope (MIRA3TESCAN-XMU) was used to find out the morphology and the dimensions of our nanowire samples. Figure 1 shows the image of as-prepared  $\alpha\text{-MnO}_2$  sample. After that, our optical composite has been prepared by polydimethylsiloxane (PDMS) polymer (Sylgard 184) from Dow Corning was used. It consists of a siloxane base and a curing agent which must be mixed in 10:1 volumetric ratio.  $\alpha\text{-MnO}_2$  NWs were mixed with the PDMS base at about 0.05 wt%. The dispersion of NWs has been done in two steps; first the mixture of PDMS base and  $\alpha\text{-MnO}_2$  NWs was sonicated for an hour at room temperature and then it was mixed mechanically by a DC motor for 30 min. Before the final minute of mixing, the curing agent was added to the PDMS base in 1:10 volumetric ratio. Then the composite has been poured into a mold and it was placed in a vacuum for 15 min to degas. Finally, the composite was cured at 80 °C for about 2 h in a heater. During the curing process, for alignment of NWs in PDMS matrix, the composite with the thickness of 1 mm has been subjected to a magnetic field. To confirm our NWs in alpha state, we use X-ray diffraction pattern. Our optical composite has been exposed to different hydrogen gas in our home-made chamber (Fig. 2). The sample was placed on a cylindrical prism by index matching gel in vacuum. Then, a sample was positioned into a gas chamber under the

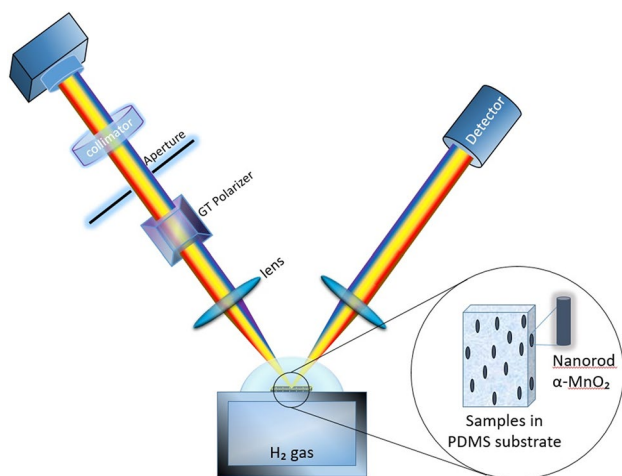


Fig. 1 Schematic diagram of the sensing experimental setup

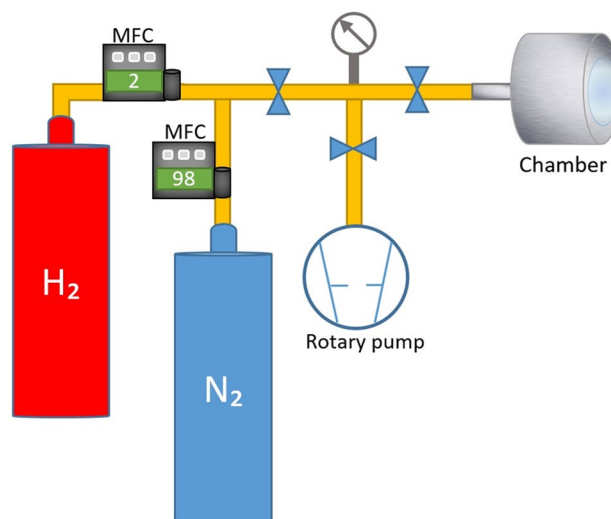


Fig. 2 Schematic diagram of the static gas volumetric method to fill gas in a chamber

flow of dry nitrogen to remove any unwanted composition from its surface. Finally, the spectral response of the sample to different injections of  $\text{H}_2$  gas has been recorded in our experimental setup as shown in Fig. 1.

The optical branch consisted of P- or S-polarized visible light which can be obtained by Glan–Taylor prism, sensor head and a spectrometer to record the response at various incident angles.

For hydrogen gas sensing confirmation, we use our ellipsometry quantity [19] as  $\psi_{\text{eff}} = \frac{\psi_{\text{H}_2} - \psi_{\text{N}_2}}{\psi_{\text{H}_2} + \psi_{\text{N}_2}}$  in each gas concentration. In this parameter,  $\psi_{\text{N}_2}$  and  $\psi_{\text{H}_2}$  introduce ellipsometry parameter at pure  $\text{N}_2$  and composition of  $\text{H}_2$  and  $\text{N}_2$  gas, respectively. In fact, to evaluate the sensing performances of the sample as  $\text{H}_2$  gas sensor, we use the static volumetric method to fill our gas chamber by injecting known volumes of standard  $\text{H}_2$  gas into a chamber equipped with  $\text{N}_2$  Gas by two mass flow controller (MFC) devices (Fig. 2).

For this step, the first MFC coupled to the  $\text{H}_2$  capsule was set to 2, 8 and 20 standard cubic centimeters per minute (SCCM) and the second ones were set to 400 SCCM for  $\text{N}_2$  gas which these amounts yields to 0.5, 2 and 5% of  $\text{H}_2$  gas in a chamber. In fact, we have 4800 part per million (ppm), 19,000 and 47,000 ppm for above mentioned  $\text{H}_2$  percent, respectively (Fig. 3).

### 3 Results and discussions

The X-ray pattern of  $\alpha\text{-MnO}_2$  phase is presented in Fig. 4 which indicates the formation of the  $\alpha\text{-MnO}_2$  tetragonal phase [space group:  $I4/m (87)$ ] that is according to JCPDS

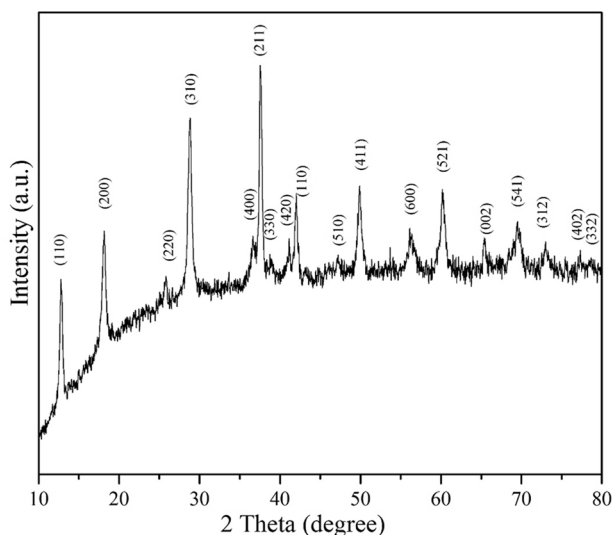


**Fig. 3** The X-ray of  $\alpha$ -MnO<sub>2</sub> prepared nanowires

data No. 44–0141 with no addition peaks of impurity. MnO<sub>2</sub> nanowires are well crystallized in the [211] lattice plane that has the most intensity. The average crystalline size was measured by Scherer formula:

$$D = \frac{k\lambda}{\beta \cos \theta} \tag{1}$$

where  $k=0.9$  is factor shape,  $\lambda=1.5406 \text{ \AA}$ ,  $\beta$  is the full-width at half maximum in radian and  $\theta$  is the angle on the maximum of the diffraction peak. Using the above formula, the average crystalline size was calculated to be 22 nm.

Figure 4 shows the image of as-prepared  $\alpha$ -MnO<sub>2</sub> sample. The length and diameter of our nanowires are in the range of about 388–2055 nm and 25–58 nm, respectively, that is measured by image j software. (with about 50 numbers).

Afterward, our optical composite has been examined in different hydrogen gas concentration. For this purpose, we measured and calculated the optical ellipsometry parameters of the sample in each concentration of H<sub>2</sub> gas. At the first step, we measure the reflectance of the sample under N<sub>2</sub> gas and calculate ellipsometric parameters as shown in Fig. 5. In this measurement, the incidence angle of P- and S-polarized light was set to 20°.

At second step, the reflectance spectra of the sensor head was recorded with respect to different injections of H<sub>2</sub> gas (0.5, 2 and 5%) and the effective plasmonic ellipsometry as  $\frac{\psi_{H_2} - \psi_{N_2}}{\psi_{H_2} + \psi_{N_2}}$ . One can see the change in this effective parameter as a function of wavelength in different H<sub>2</sub> gas concentrations (Fig. 6a). The main peak of effective parameter has blue shift under different gas concentrations which confirms that the composite sample has a good sensitivity to different hydrogen gas concentrations in all of the visible regions (Fig. 6b).

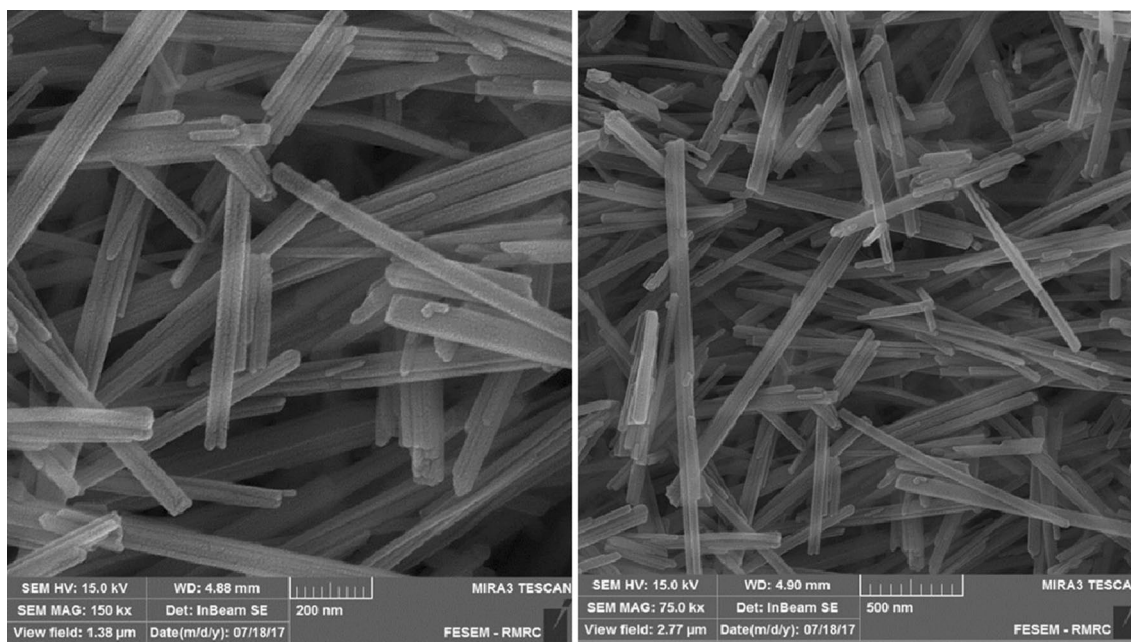


**Fig. 4** SEM image of prepared  $\alpha$ -MnO<sub>2</sub> nanowires with two different magnifications, 500 and 200 nanometer

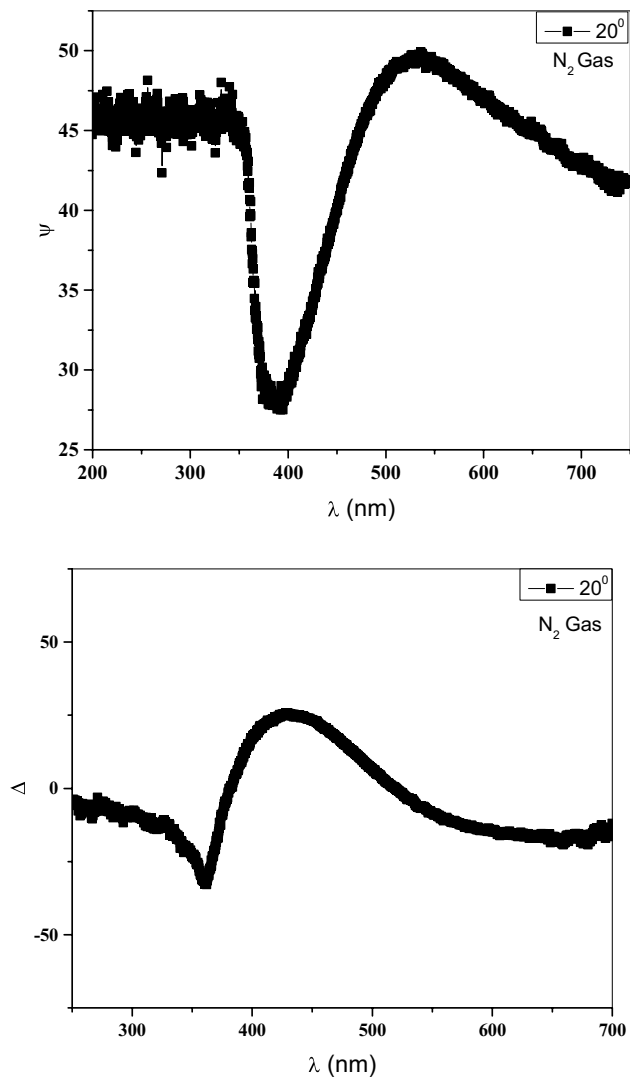


**Fig. 5** Ellipsometric parameters of sample under pure  $N_2$  gas at  $20^\circ$  incidence angle

In addition, we have efficient change in the effective ellipsometry parameter as a function of different gas concentrations as can be seen in Fig. 6c.

Thanks to the efficient crystalline nature of  $\alpha$ - $MnO_2$  nanowires and also the high aspect ratio of them, we see sufficient sensitivity to the different hydrogen gas concentrations. In fact, due to much more free space between each nanowire and also above-mentioned high aspect ratio, we have two main reason for  $H_2$  gas sensing. The first one is efficient site to absorb the gas between nanowires and the second one is the large surface to volume ratio of each nanowire.

Now based on the ellipsometric parameters such as the psi and delta, we can measure the change in the refractive indices of the samples under different gas concentrations. One may know that in PDMS matrix we have efficient oxygen concentrations as shown in Fig. 7.

For this reason, we have the potential of initial  $H_2O$  composition due to the exposure of the sample under  $H_2$  gas purge and then produce the  $Mn(III)OO\cdot H$  in the sample's surface. On the other word, we expect that the role of oxygen in the PDMS is the change of the surface composition from  $MnO_2$  to  $Mn(III)OO\cdot H$  with the effect of water oxidation (which is approved in  $MnO_2$  materials [12]) and thus the change in the refractive index; the phase of the reflectance and, therefore, the ellipsometric parameters.

## 4 Conclusions

Overall, we have synthesized the high aspect ratio  $\alpha$ - $MnO_2$  nanowires by the aid of hydrothermal effect and dispersed them into transmittive polymeric media to use them as an efficient hydrogen gas sensor. Our sample has been examined under different gas concentrations from 0 to 5% in vacuum chamber. The results indicate the logic change in the sample's response according to the different gas concentrations and one can see the linear behavior of resonance wavelength in ellipsometric parameter as a function of gas concentrations which indicate the sample's capability for hydrogen gas sensing practical applications.

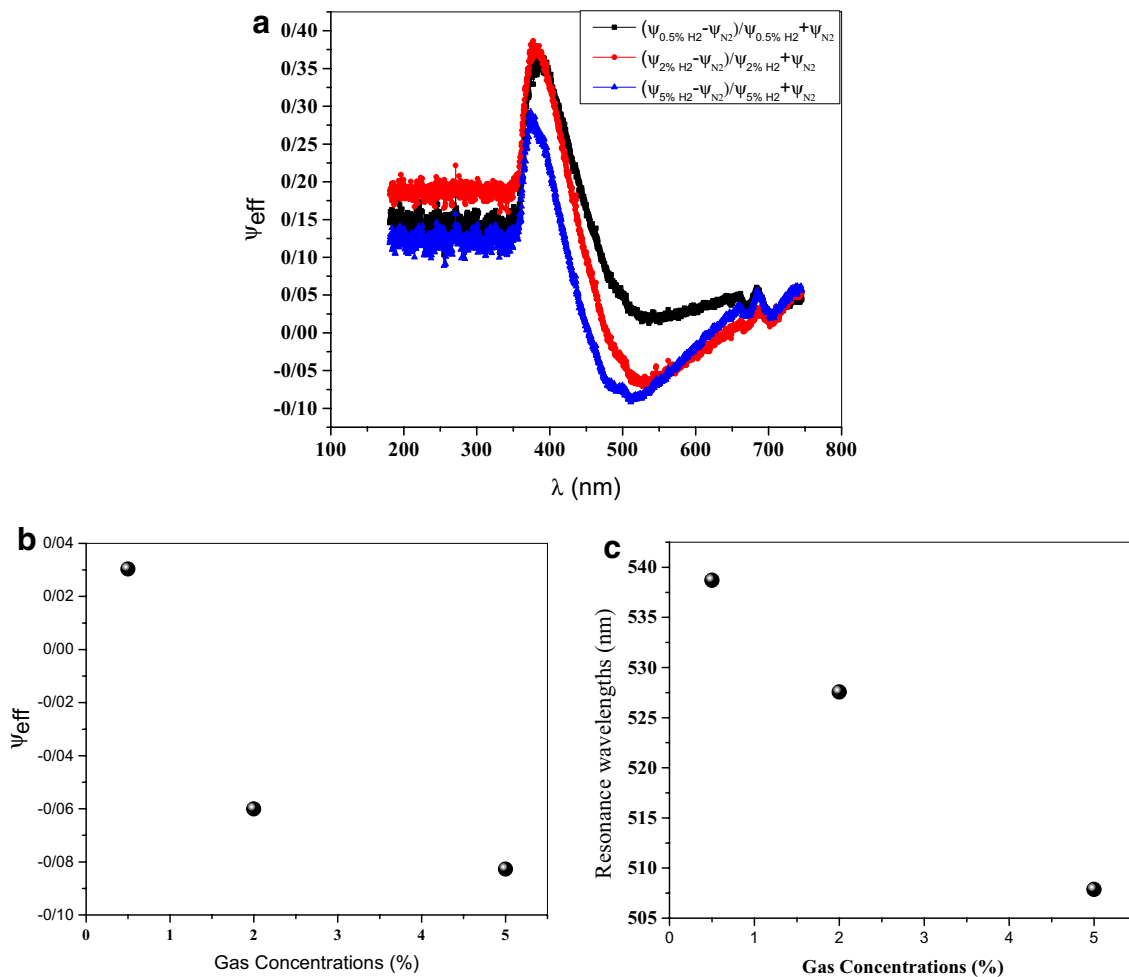


**Fig. 6** **a** Ellipsometric effective parameter of the sample under different H<sub>2</sub> gas concentrations, **b** main peak of effective parameter and **c** resonance wavelength as a function of Gas concentrations

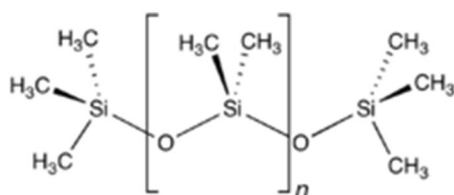


**Fig. 7** The chemical structure of the ePDMS matrix

## References

- H. Waechter, J. Litman, A.H. Cheung, J.A. Barnes, H.P. Loock, Chemical sensing using fiber cavity ring-down spectroscopy. *Sensors* **10**, 1716 (2012)
- E. Vargas-Rodríguez, H.N. Rutt, Design of CO, CO<sub>2</sub> and CH<sub>4</sub> gas sensors based on correlation spectroscopy using a Fabry–Perot interferometer. *Sens. Actuators B* **137**, 410 (2009)
- R.R. Rye, A.J. Ricco, Ultrahigh vacuum studies of Pd metal-insulator-semiconductor diode H<sub>2</sub> sensors. *J. Appl. Phys.* **62**, 1084 (1987)
- S. Shukla, P. Zhang, H.J. Cho, L. Ludwig, S. Seal, Significance of electrode-spacing in hydrogen detection for tin oxide-based MEMS sensor. *Int. J. Hydrogen Energy* **33**, 470 (2008)
- S.M. Hamidi, R. Ramezani, A. Bananej, Hydrogen gas sensor based on long-range surface plasmons in lossy palladium film placed on photonic crystal stack. *Opt. Mater.* **53**, 201 (2016)
- N.R. Fong, P. Berini, R.N. Tait, Modeling and design of hydrogen gas sensors based on a membrane-supported surface Plasmon waveguide. *Sens. Actuators B* **161**, 285 (2012)
- F. Gu, H. Zeng, Y.B. Zhu, Q. Yang, L.K. Ang, S. Zhuang, Single crystal Pd and its alloy nanowires for Plasmon propagation and highly sensitive hydrogen detection. *Adv. Opt. Mater.* **2**, 189 (2014)
- M. Huang, F. Li, F. Dong, Y.X. Zhang, L.L. Zhang, MnO<sub>2</sub>-based nanostructures for high-performance supercapacitors. *J. Mater. Chem. A* **3**, 21380–21423 (2015)
- X. Tiana, L. Yang, X. Qing, K. Yu, X. Wang, Trace level detection of hydrogen gas using birnessite-type manganese oxide. *Sens. Actuators B* **207**, 34 (2015)

10. Y. Uedaa, A.I. Kolesnikov, H. Koyanaka, Sensing hydrogen gas concentration using electrolyte made of proton conductive manganese dioxide. *Sens. Actuators B* **155**, 893 (2011)
11. Y. Ueda, Y. Tokuda, T. Yoko, K. Takeuchi, A.I. Kolesnikov, H. Koyanaka, Electrochemical property of proton-conductive manganese dioxide for sensing hydrogen gas concentration. *Solid State Ionics* **225**, 282 (2012)
12. H. Koyanaka, Y. Ueda, K. Takeuchi, A.I. Kolesnikov, Effect of crystal structure of manganese dioxide on response for electrolyte of a hydrogen sensor operative at room temperature. *Sens. Actuators B* **183**, 641 (2013)
13. Y. Ueda, Y. Tokuda, T. Yoko, K. Takeuchi, A.I. Kolesnikov, H. Koyanaka, Electrochemical property of proton-conductive manganese dioxide for sensing hydrogen gas concentration. *Solid State Ionics* **225**, 282 (2012)
14. J. Xiao, P. Liu, Y. Liang, H.B. Li, G.W. Yang, High aspect ratio  $\beta$ -MnO<sub>2</sub> nanowires and sensor performance for explosive gases. *J. Appl. Phys.* **114**, 073513 (2013)
15. X. Tian, L. Yang, X. Qing, K. Yua, X. Wang, Trace level detection of hydrogen gas using birnessite-type manganese oxide. *Sens. Actuators B* **207**, 34 (2015)
16. J. Xiao, P. Liu, Y. Liang, H.B. Li, G.W. Yang, High aspect ratio  $\beta$ -MnO<sub>2</sub> nanowires and sensor performance for explosive gases. *J. Appl. Phys.* **114**, 073513 (2013)
17. M. Musil, B. Choi, A. Tsutsumi, Morphology and electrochemical properties of  $\alpha$ -,  $\beta$ -,  $\gamma$ -, and  $\delta$ -MnO<sub>2</sub> synthesized by redox method. *J. Electrochem. Soc.* **162**, 2058 (2015)
18. W. Tang, X. Shan, S. Li, H. Liu, X. Wu, Y. Chen, Sol-gel process for the synthesis of ultrafine MnO<sub>2</sub> nanowires and nanorods. *Mater. Lett.* **132**, 317 (2014)
19. F. Sohrabi, S.M. Hamidi, Optical detection of brain activity using plasmonic ellipsometry technique. *Sens. Actuators B* **251**, 153 (2017)